Photochemistry of Methanol and Methoxy Groups Adsorbed on Powdered TiO_2

Chih-Chung Chuang, Chih-Cheng Chen, and Jong-Liang Lin*

Department of Chemistry, National Cheng Kung University, Tainan, Taiwan, Republic of China

Received: September 16, 1998; In Final Form: December 8, 1998

The photochemistry of $CH_3OH_{(a)}$ and $CH_3O_{(a)}$ adsorbed on TiO_2 and the effect of O_2 have been studied by infrared spectroscopy and mass spectrometry. In the absence of O_2, $CH_3OH_{(a)}$ desorbs molecularly, while $CH_3O_{(a)}$ decomposes to form $CH_2O_{(g)}$ under UV irradiation. The rate of $CH_3O_{(a)}$ decomposition reaches maximum in the initial stage of UV irradiation and then decreases significantly. On the other hand, for the reaction in O_2, the behavior of $CH_3O_{(a)}$ depletion upon UV irradiation is very different, giving rise to adsorbed $HCOO_{(a)}$ and $H_2O_{(a)}$. A radical mechanism is proposed to explain the variation of $CH_3O_{(a)}$ depletion upon UV irradiation, the role of O_2, and the formation of the reaction products.

Introduction

Studies of adsorption and reactions of alcohols on TiO_2 are of interest in making materials of industrial importance, understanding the reaction elementary steps for the formation of TiO_2 by chemical vapor deposition using titanium alkoxide precursors, and transforming organic pollutants into innocuous products photochemically. Several studies of methanol on TiO_2 including surface bonding,[1−4] thermal reactions,[3−5] and photo-induced oxidation of methanol on TiO_2 have been reported. The focus in the photooxidation experiments consisted of studies of catalytic conversion and selectivity,[6] the effect of metal ions,[7] the role of photogenerated electron−hole pairs,[8,9] and the characteristics of photogenerated paramagnetic intermediates.[10] These experiments were carried out with TiO_2 particles in contact with methanol either in solution or in the gas phase without providing detailed adsorption information. Since the photoreactions on TiO_2 are initiated by electron−hole pairs from band gap excitation, the state and adsorption of the surface must play an important role in determining the reaction pathways and their kinetics. Taylor et al. have previously studied the photochemistry of TiO_2 surfaces following CH_3OH adsorption in the absence of O_2.[3] Reaction products, including H_2O, CO, H_2, CH_3OH, CH_2O, CH_4, and CO_2, were observed. It was found that all of the product fluxes quickly decreased to one-half of their initial values within 3−5 min upon UV irradiation. Unfortunately, in this study, detailed information of surface coverage, UV wavelength, UV power, and surface temperature during UV irradiation was not provided. Possible mechanisms for the formation of the various products were not discussed either.

In the present study, through a control of the surface concentration of adsorbed species on TiO_2, we study the photochemistry of adsorbed methanol and methoxy groups in the absence of O_2 by in situ FTIR spectroscopy and mass spectrometry during UV irradiation and make a comparison with the results in the presence of O_2. Operative mechanisms in these reactions are discussed.

* To whom the correspondence should be addressed. Department of Chemistry, National Cheng Kung University, 1, Ta Hsueh Rd., Tainan, Taiwan, ROC. E-mail: jonglin@mail.ncku.edu.tw. Fax: 011-886-6-2740552.

Experimental Section

The details of stainless steel IR cell with two CaF_2 windows for IR transmission down to 1000 cm^{-1} has been reported previously.[11] The IR cell was connected to a gas manifold which was pumped by a 60 L/s turbo-molecular pump with a base pressure of $\sim 1 \times 10^{-7}$ Torr. The TiO_2 sample was supported on a tungsten grid held in a pair of stainless steel clamps which were attached to the power leads of a power/thermocouple feedthrough. The sample temperature was measured by a K-type thermocouple spot welded on the tungsten grid, raised by passing electric current through the grid, and controlled by a temperature controller. The TiO_2 sample on tungsten grid was prepared according to the similar procedure as reported previously.[12] In brief, TiO_2 powder (Degussa P25, $\sim$50 m^2/g, anatase 70%, rutile 30%)[13] was well dispersed in water/acetone solution to form a uniform mixture, which was then sprayed onto the entire area of the tungsten grid. The TiO_2 sample was then mounted in the IR cell for simultaneous photochemistry and FTIR spectroscopy, with both the IR beam from the FTIR spectrometer and the UV beam from the Hg arc lamp emitting at 45° to the normal of the tungsten grid. The sample in the IR cell was then outgassed at 450 °C under vacuum for 24 h. Before each run of the experiment, the TiO_2 sample was heated to 450 °C for 2 h and cooled back to $\sim$35 °C for gas dosing. O_2 (99.998%) was purchased from Matheson. Methanol (99.8%) was obtained from BDH Laboratory Supplies and purified by several cycles of freeze−pump−thaw before introduction to the cell. Pressure was monitored with a Baratron capacitance manometer and an ion gauge. The UV light source used was a 350 W Hg arc lamp (Oriel corp). A water filter and a band-pass filter (320 ± 60 nm) were used in this study. The power at the position of the TiO_2 sample was $\sim$0.24 W/cm^2 measured in the air by a power meter (Molectron, PM10V1). Infrared spectra were obtained with 4 cm^{-1} resolution by Bruker FTIR spectrometer with a MCT detector. The entire optical path was purged with CO_2-free dry air. In the case of gas analysis during photoirradiation of the TiO_2 sample using a quadrupole mass spectrometer (Stanford Research System, 200 amu), the same sample cell for FTIR studies was used and evacuated with a 250 L/s turbo-molecular pump. Both the QMS and the UV beams were held 45° to the normal of the tungsten grid. The QMS was

10.1021/jp983750s CCC: $18.00 © 1999 American Chemical Society
Published on Web 03/16/1999

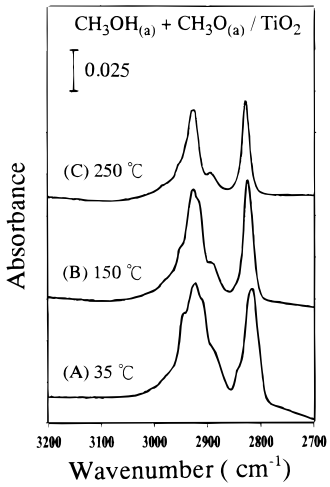

Figure 1. Infrared spectra of a TiO_2 surface exposed to 2 Torr of CH_3OH and then evacuated at the indicated temperatures for 1 min. All the spectra were recorded with 100 scans at 35 °C

multiplexed for 10 masses, i.e., 10 ions were simultaneously recorded as a function of photoirradiation time under vacuum.

Results

The previous IR study by Taylor and Griffin[3] has demonstrated temperature-dependent CH_3OH adsorption on TiO_2. CH_3OH adsorbs on TiO_2 in two forms: molecular $CH_3OH_{(a)}$ and dissociatively chemisorbed $CH_3O_{(a)}$ groups. The stretching bands of CH_3 of $CH_3OH_{(a)}$ appear at 2950 and 2850 cm^{-1}, while those of $CH_3O_{(a)}$ appear at 2930 and 2830 cm^{-1}. Similar results were observed in this study. After exposing 2 Torr of CH_3OH to a clean TiO_2 sample and evacuated at 35 °C, an infrared spectrum was recorded, as shown in Figure 1A. The characteristic absorption of both adsorbed $CH_3OH_{(a)}$ and $CH_3O_{(a)}$ were seen. In this spectrum the peak intensity of 2950 cm^{-1} is ∼75% of that of 2930 cm^{-1}. Figure 1B and C shows the spectra after the TiO_2 temperature was raised to 150 and 250 °C under vacuum, respectively. When the temperature was raised, part of the $CH_3OH_{(a)}$ desorbed and the rest underwent a dissociative conversion to $CH_3O_{(a)}$. This effect can be seen in the decrease of the peak intensity ratio of 2950 cm^{-1} to 2930 cm^{-1}: it becomes roughly ∼50% at 150 °C and ∼30% at 250 °C. These values imply that for each $CH_3O_{(a)}$ group on the TiO_2 surface the number ratio of the $CH_3OH_{(a)}$ for the TiO_2 sample at 35, 150, and 250 °C is roughly 2.5:1.7:1, assuming the peak intensity is proportional to the surface concentration of the adsorbed groups. Note that these numbers by no means represent the absolute numbers of adsorbed $CH_3OH_{(a)}$ per $CH_3O_{(a)}$. The TiO_2 evacuated at 250 °C is basically covered with $CH_3O_{(a)}$ and small amounts of residual $CH_3OH_{(a)}$. Using the previously reported adsorption isotherms of methanol on TiO_2[1,2] and assuming equal infrared extinction coefficients for the $CH_3O_{(a)}$ and $CH_3OH_{(a)}$, the surface concentration of $CH_3O_{(a)}$ at this temperature is estimated roughly to be ∼1.3 molecules/nm^2. Small quantities of $CH_3O_{(a)}$ may react on the TiO_2 surface to form $CH_3OCH_{3(g)}$ and $CH_2O_{(g)}$ at 250 °C.[3−5] It gives rise to smaller peak intensities of 2830 and 2930 cm^{-1} as compared to those at 150 °C.

Figure 2A shows the infrared spectra of a TiO_2 surface, which was first treated with 2 Torr of CH_3OH followed by evacuation at 250 °C for 1 min, in a closed cell before UV irradiation, for 30 and 150 min during UV irradiation in the absence of O_2. In the IR spectrum taken before UV irradiation, the surface hydroxyl signals shown in the region of 3500−3800 cm^{-1} decrease, as compared to a clean TiO_2 surface. Absorptions

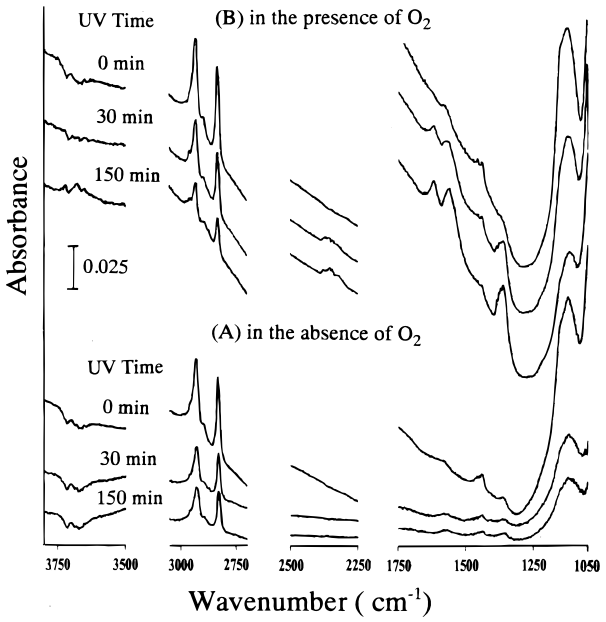

Figure 2. Infrared spectra of TiO_2 samples adsorbed with $CH_3OH_{(a)}$ and $CH_3O_{(a)}$ before irradiation, for 30 and 150 min during UV irradiation in a closed cell without (A) O_2 and in the presence of (B) 10 Torr of O_2. The TiO_2 sample was prepared by exposing 2 Torr of CH_3OH to a clean TiO_2 surface and then evacuating at 250 °C for 1 min. All the (A) spectra have been ratioed against a clean TiO_2 spectrum. In the presence of O_2, due to the oxygen adsorption on the surface, there is a weak, broad absorption feature between 1250 and 1650 cm^{-1} which changes slightly with UV irradiation. Therefore, each (B) spectrum has been ratioed against the corresponding spectrum of a clean TiO_2 surface in 10 Torr of O_2 under the same amount of UV irradiation time. To represent the dynamic behavior, each spectrum was obtained with 5 scans.

related to the $CH_3O_{(a)}$ including the CH_3 stretching in the region of 2750−3000 cm^{-1}, CH_3 bending and C−O stretching in 1050−1750 cm^{-1} are also shown.[4] During the period of the UV irradiation, no new surface IR features appear other than the decrease of the absorption bands from the adsorbed groups. Similar results were obtained for the TiO_2 surface treated with CH_3OH and evacuated at 150 °C. Both the loss of the $CH_3O_{(a)}$ and $CH_3OH_{(a)}$ and the lack of new IR bands upon UV illumination can be attributed to the desorption of the adsorbed species, although the desorption products are not detectable by our IR spectrometer. The decrease of relative $CH_3O_{(a)}$ concentration, expressed by the normalized peak area calculated from 2800 to 2850 cm^{-1}, with photoirradiation time is shown in Figure 3A. $CH_3O_{(a)}$ has a large extent of reduction (∼50%) within 500 s after the lamp is turned on and further decay takes much longer time. From the slope of the $CH_3O_{(a)}$ decreasing curve, the maximum rate appears at ∼60 s. During the UV irradiation, the TiO_2 temperature increased to ∼110 °C, so a separate control experiment was carried out to check the possibility of thermal effect. There was no decrease of $CH_3O_{(a)}$ as the TiO_2 sample was held at 110 °C for 150 min, indicating that the diminution of $CH_3O_{(a)}$ in this photoillumination experiment is not a result of thermal heating. To detect the desorption products induced by the UV irradiation of the TiO_2, a QMS was used for monitoring a mass range of 1 to 60 amu when the TiO_2 sample was illuminated by the UV light. Figure 4A shows the major detected ions of the photostimulated products under vacuum from the adsorbed $CH_3O_{(a)}$ and $CH_3OH_{(a)}$ on the TiO_2 surface prepared by CH_3OH adsorption and then evacuation at 250 °C. At a pumping speed as high as that used in this study, the ion intensities recorded by QMS are proportional to

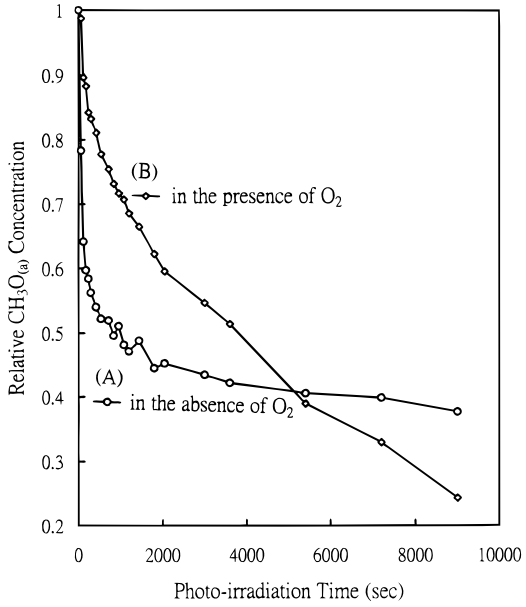

Figure 3. Relative concentration of $CH_3O_{(a)}$ as a function of UV irradiation time in the absence of (A) O_2 and in the presence of (B) 10 Torr of O_2. The TiO_2 sample was prepared by exposing 2 Torr of CH_3OH to a clean TiO_2 surface and then evacuating at 250 °C for 1 min. The zero second of the photoirradiation time represents the time that Hg lamp is turned on. It takes ~40−45 s to reach a full power of the lamp.

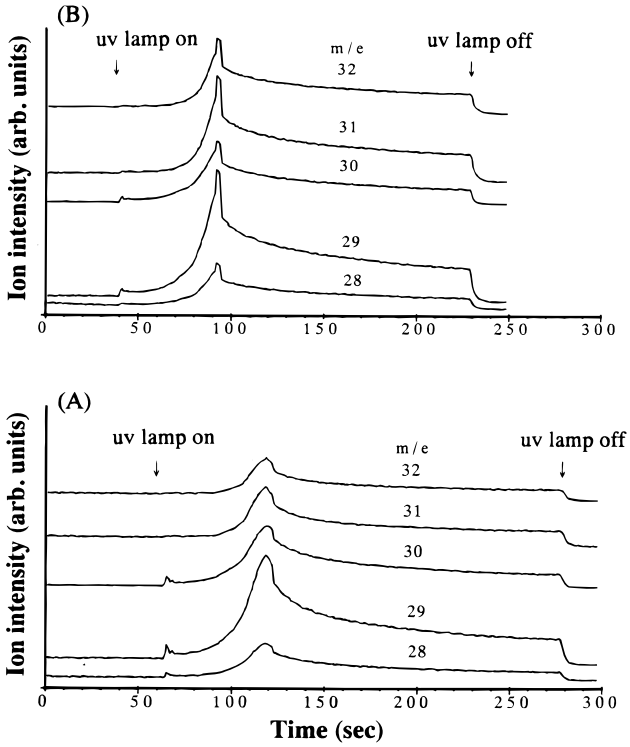

Figure 4. Major detected ions of the photoinduced reaction/desorption products from TiO_2 surfaces adsorbed with $CH_3OH_{(a)}$ and $CH_3O_{(a)}$. The TiO_2 samples were prepared by exposing 2 Torr of CH_3OH to a clean TiO_2 sample and then evacuating at (B) 150 °C or (A) 250 °C for 1 min.

the desorption rate.[14] All the masses in Figure 4A concurrently reach the ion current maxima, i.e., the maximum desorption rate, at ~50−55 s after the UV lamp is turned on, and then gradually decrease. This result is consistent with the FTIR study in Figure 2A and 3. The disappearance rate of $CH_3O_{(a)}$ monitored by FTIR during the UV irradiation matches well to

TABLE 1: Analysis of Photoinduced Products

ions (amu)	ion intensity	ion intensity after subtracting CH_3OH contribution	CH_3OH^a	CH_2O^b
32	35		73	
31	48		100	
30	57	49 (64)	16	66
29	100	76 (100[c])	50	100
28	22	24 (32)	19	33

[a] This work. [b] From ref 15. [c] Mass 29 amu is scaled to 100 for comparison.

the product formation rate of the photoinduced desorption. The ions observed in Figure 4A and their normalized intensities are listed in the first two columns of Table 1. As to the identity of the photoinduced desorption products, the detected highest mass at 32 amu (CH_3OH^+) in Figure 4A reveals the desoption of $CH_3OH_{(g)}$. This assignment is also supported by the intensity ratio of the 32 amu to the 31 amu ($I_{m/e=32}/I_{m/e=31} = 0.73$), which is consistent with that of the gas-phase CH_3OH detected by our QMS (see the fourth column of Table 1). Although CH_3OH has a cracking pattern at 30, 29, and 28 amu, CH_3OH alone cannot account for the entire fragment pattern in Figure 4A. To further identify the other possible photoinduced products, subtraction of the methanol contribution from the second column of Table 1 has been made. The remaining relative ion intensities shown in the third column agree with the standard mass spectrum of CH_2O (see the last column in Table 1). In addition, small amounts of H_2O and H_2 were also found, but not shown here. Figure 4B shows the similar results for a TiO_2 sample prepared by CH_3OH adsorption and then evacuation at 150 °C. It is informative to further study the correlation between the concentrations of $CH_3OH_{(a)}$ relative to $CH_3O_{(a)}$ and the photoinduced desorption signals of $CH_3OH_{(g)}$ relative to $CH_2O_{(g)}$. The relative yield ratio of 31 amu from $CH_3OH_{(g)}$ to 30 amu from $CH_2O_{(g)}$ is ~0.98 for the TiO_2 sample evacuated at 250 °C. On the other hand, for the TiO_2 sample evacuated at 150 °C, the ion yield ratio of 31 amu from $CH_3OH_{(g)}$ to 30 amu from $CH_2O_{(g)}$ becomes ~2.2. These values can be interpreted to be that, for the formation of each $CH_2O_{(g)}$ molecule, the number ratio of $CH_3OH_{(g)}$ desorbed from the TiO_2 sample evacuated at 150 °C to that at 250 °C is roughly 2.2/0.98 = 2.2. It is worth noting that, on the basis of the IR study mentioned above for each $CH_3O_{(a)}$ on the TiO_2 surface, the number ratio of $CH_3OH_{(a)}$ on the TiO_2 sample evacuated at 150 °C to that at 250 °C is roughly 1.7. This reveals that the more $CH_3OH_{(a)}/CH_3O_{(a)}$ is adsorbed on the surface, the more $CH_3OH_{(g)}/CH_2O_{(g)}$ is desorbed.

In contrast, in the presence of O_2, the adsorbed $CH_3O_{(a)}$ groups behave very differently under UV irradiation in the rate of $CH_3O_{(a)}$ depletion and in the change of adsorption on the TiO_2 surface. Figure 2B shows the infrared spectra of the TiO_2 surface, previously treated with 2 Torr of CH_3OH followed by evacuation at 250 °C, irradiated in the presence of 10 Torr of O_2 for 0, 30, and 150 min. New bands appear at 1370, 1565, and 1620 cm^{-1} and grow simultaneously with the UV irradiation at the expense of $CH_3O_{(a)}$. These new bands are attributed to adsorbed $HCOO_{(a)}$ (1370 cm^{-1}, 1565 cm^{-1}) and $H_2O_{(a)}$ (1620 cm^{-1}). In addition, the appearance of $CO_{2(g)}$ band shown in 2250−2500 cm^{-1} and the increase of isolated hydroxyl absorption are observed. The $CO_{2(g)}$ formation and the increasing $OH_{(a)}$ concentration are due to $HCOO_{(a)}$ photoreaction[16,17] and $H_2O_{(a)}$ decomposition, respectively. Since the temperature increased to ~90 °C during the UV irradiation, a separate control experiment was carried out by holding the surface temperature

at 90 °C for 150 min. In this experiment it was found that the IR intensity of CH_3 stretching of $CH_3O_{(a)}$ remained almost constant while only very weak absorption of $HCOO_{(a)}$ appeared, and its intensity was <7% of that obtained from UV irradiation. Therefore, it is concluded that the thermal effect is small, if it exists. Figure 3B shows the decrease of $CH_3O_{(a)}$ concentration as a function of UV irradiation time in O_2. In O_2 the $CH_3O_{(a)}$ decreasing behavior is very different from that in the absence of O_2. It does not reduce significantly in the initial stage of UV irradiation and decreases more thoroughly after prolonged irradiation. To check the effects of the possible light scattering and/or slight absorption of the 320 nm photons by the gas-phase O_2[18] on the photon flux received by the TiO_2 sample, a calibration experiment to compare the power after the UV light passing through the cell in a vacuum or in the presence of 10 Torr of O_2 was carried out. In this experiment, the measured powers in both cases are the same within the detection uncertainty. Therefore, the slower $CH_3O_{(a)}$ initial depletion rate in the presence of O_2 likely originates from the adsorbed O_2 which alters the photoexcitation process. Both the continuing significant $CH_3O_{(a)}$ depletion rate at prolonged UV irradiation and the formation of new surface species in the presence of O_2 imply other reaction pathways exist.

Discussion

This section is composed of two major parts. First, we discuss the states of the TiO_2 surface formed by our sample preparation procedures and experimental conditions. Second, we propose reaction mechanisms to interpret the different types of photoreactions of $CH_3O_{(a)}$ on TiO_2 with and without O_2. TiO_2 is a semiconductor with ~3.1 eV (400 nm) band gap. On evacuation at ~500 °C, TiO_2 powders retain partial $OH_{(a)}$ groups on the surface[3,4] and lose part of O atoms to form F-centers[19] and Ti^{3+} [19,20] as concluded by electron spin resonance studies. Upon irradiation with UV light at 3.4 eV, Ti^{3+} defects are enhanced on a nearly defect-free TiO_2(110) single-crystal surface as evidenced by X-ray photoelectron spectroscopy.[21] The enhancement of Ti^{3+} may also take place on powdered TiO_2 samples under UV illumination. In the presence of O_2, adsorbed O_2 reacts with either F-centers[19] or Ti^{3+} [20] giving rise to O_2^-. On annealed TiO_2 surfaces upon UV irradiation at 77 K, ESR has shown the existence of O_3^-, O_3^{-3}, and O_2^- species. However, only O_2^- is shown to be stable at room temperature.[22]

As CH_3OH is adsorbed on the TiO_2 surface previously annealed at 450 °C, it readily decomposes to form $CH_3O_{(a)}$ and $H_2O_{(g)}$ upon surface heating to 250 °C in a vacuum. The $H_2O_{(g)}$ formation is due to the reaction between the protons from dissociated $CH_3OH_{(a)}$ and residual $OH_{(a)}$ groups on the TiO_2 surface,[3] as evidenced by the diminution of surface $OH_{(a)}$ groups in Figure 2A as compared to that on a clean TiO_2 surface. Upon UV irradiation on the TiO_2 surface adsorbed with $CH_3O_{(a)}$ and residual $CH_3OH_{(a)}$ in the absence of O_2, desorption of CH_3OH, CH_2O, H_2O, and H_2 is detected by mass spectrometry. The formation of $CH_3OH_{(g)}$ and $CH_2O_{(g)}$ is presumably due to the photoinduced desorption/reaction of the adsorbed species. By studying the correlation between the relative product yields and the concentrations of the surface species during the UV irradiation, it is found that the more the formation of $CH_3OH_{(a)}$/$CH_3O_{(a)}$ increases, which is controlled by annealing temperature after CH_3OH adsorption, the more the desorption of $CH_3OH_{(g)}$/$CH_2O_{(g)}$ increases. This finding strongly suggests that $CH_3OH_{(g)}$ production is due to the photodesorption of $CH_3OH_{(a)}$ and $CH_2O_{(g)}$ is mainly from the photoreaction of $CH_3O_{(a)}$. Although the possibility of $CH_3OH_{(g)}$ from $CH_3O_{(a)}$ and $CH_2O_{(g)}$ from $CH_3OH_{(a)}$ cannot be completely ruled out, their contributions are minor if they do occur in this study. $CH_3O_{(a)}$ photodecomposition may occur by directly absorbing UV photons or through TiO_2 band-gap excitation. If the former is the operative mechanism, the surface concentration of $CH_3O_{(a)}$ is expected to decrease exponentially with UV irradiation time. However, it is not consistent with the results observed in this study. The photodecomposition of $CH_3O_{(a)}$ is therefore caused by TiO_2 band-gap excitation, i.e., by photogenerated electron−hole pairs in the absence of O_2. On the other hand, if O_2 is present, the direct excitation of O_2 is possible within the UV wavelength range of the present study.[18] However, in the study of CH_3Cl photooxidation on a TiO_2(110) single-crystal surface, on the basis of the results of photon energy-dependent reactant consumption, Lu et al. has concluded that TiO_2 mediated excitation is the dominant process.[23]

Micic et al. have studied the photoreactions of aqueous methoxide/TiO_2 colloids in the absence of O_2 by ESR to detect radical intermediates.[10] Under the pulsed laser irradiation at 308 nm, 2.5 mJ/pulse, the recorded ESR signal of $g = \sim 2$ at 6 K is assigned to $-OCH_2^{\bullet}$ radicals whose spectral features change with temperature and disappear at 150 K, doubling the intensity of Ti^{3+} signal. A radical mechanism originated from electron−hole pairs is proposed to explain the observed results.

$$Ti^{4+}-O-Ti^{4+}-OCH_3 + h^+ \rightarrow Ti^{4+}-O-Ti^{4+}-OCH_2^{\bullet} + H^+$$

$$Ti^{4+}-O-Ti^{4+}-OCH_2^{\bullet} \rightarrow Ti^{4+}-O-Ti^{3+} + CH_2O$$

$CH_3O_{(a)}$ receives photoholes to form $-OCH_2^{\bullet}$ radicals, which then ineject electrons into TiO_2 to increase the concentration of Ti^{3+}. A similar two-step mechanism has been proposed to explain the current doubling effect for the formate ($HCOO^-$) oxidation on a ZnO single-crystal electrode by electrical techniques. The formate oxidation is initiated by receiving photogenerated holes to produce formyloxy radicals ($HCOO^{\bullet}$), which then inject electrons into TiO_2 conduction band to cause current doubling.[17]

A similar radical mechanism, as shown in Scheme 1, is invoked here to explain the $CH_3O_{(a)}$ photooxidation in the present study. $CH_3O_{(a)}$ receives photoholes to form $-OCH_2^{\bullet}$ radicals followed by homolytically breaking the $Ti-OCH_2^{\bullet}$ bond and desorbs as $CH_2O_{(g)}$. In the aspect of $CH_3O_{(a)}$ photooxidation rate, Figure 3 has shown that the highest rate occurs at the beginning of UV irradiation (at ~60 s), and then the rate decreases significantly, almost down to zero for prolonged irradiation. The decreasing $CH_3O_{(a)}$ decomposition rate may be in part due to the depletion of available $CH_3O_{(a)}$ during the time of UV irradiation. Since the $CH_3O_{(a)}$ decomposition is initiated by holes, its rate must also be governed by the rate with which the photogenerated charge carriers reach the TiO_2 surface. It is well-known that photooxidation efficiency is limited by the increase of electron−hole recombination due to the accumulation of electrons on the TiO_2 surface along with photoillumination.[8] Therefore, the observed variation of $CH_3O_{(a)}$ decomposition rate with UV irradiation time in the present study can be appropriately explained by the availability of photogenerated holes at the TiO_2 surface.

In the presence of O_2, two distinct differences in the experimental results are seen, as compared to the case without O_2. One is the behavior of $CH_3O_{(a)}$ loss with UV irradiation; the other is the appearance of surface species of $H_2O_{(a)}$ and $HCOO_{(a)}$. It is known that one of the roles of O_2 in TiO_2

SCHEME 1

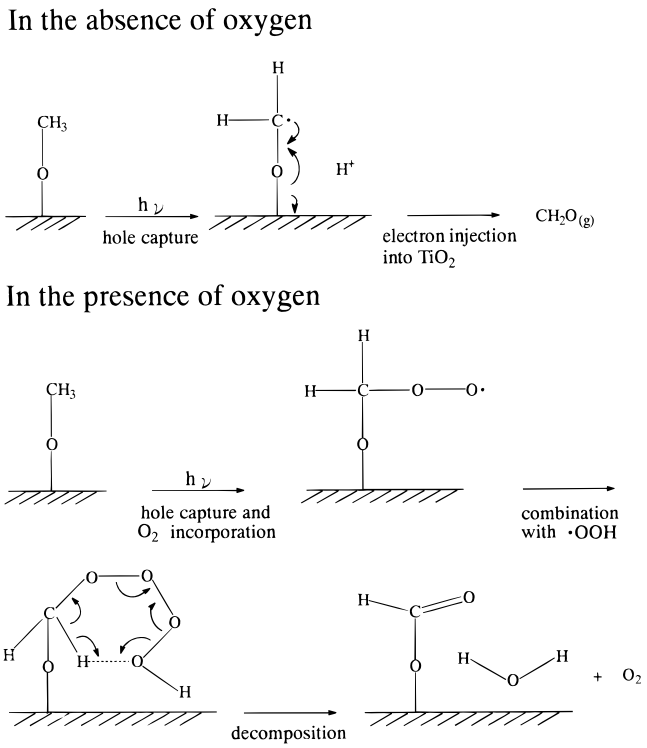

photochemistry is to capture the photoelectrons from band-gap excitation due to its high electron affinity. O_2 may also participates as a reactant in TiO_2 photochemistry. A recent study, reported by Schwitzgebel et al., of the photooxidation of C_8 organics with TiO_2-coated glass microbubbles provides this role played by O_2 in the reaction.[24] In their study, the equations of the photocatalytic reactions are able to be balanced by assuming organoperoxy and tetraoxide intermediates which originate from O_2 participation. O_2 plays two roles in the photooxidation: it receives photoelectrons and reacts with reaction intermediates as well. In terms of the possible roles of O_2, the reaction pathways proposed in Scheme 1 are used to explain the results of $CH_3O_{(a)}$ photooxidation in the absence and the presence of O_2 in the present study. In the beginning, $CH_3O_{(a)}$ receives photoholes from TiO_2 band-gap excitation and decomposes to form $-OCH_2^{\bullet}$ radical, which then dissociates to yield $CH_2O_{(g)}$ in the absence of O_2. As a contrast, in the presence O_2, the $-OCH_2^{\bullet}$ incorporates with O_2 to generate $-OCH_2OO^{\bullet}$ peroxy radicals. On the other hand, O_2 also receives electrons and then reacts with H^+ to form $HOO^{\bullet}$ radicals. The $-OCH_2OO^{\bullet}$ and $HOO^{\bullet}$ radicals then recombine to produce $-OCH_2OOOOH$ tetraoxides, which at last decompose to generate $HCOO_{(a)}$ and $H_2O_{(a)}$. The unidentate $HCOO_{(a)}$ shown in Scheme 1 may change to a bridging coordination. In the radiolysis studies of aqueous solutions of organic compounds in the presence of O_2, tetraoxides have been widely studied and proposed to be reaction intermediates.[24] Recently, Sadeghi et al. have studied the photooxidative degradation of CH_3OH vapor in contact with Pt/TiO_2 in the presence of O_2 by time-resolved photocharge measurements. On the basis of the results of the correlation between photoinduced charge carrier separation distance (CCSD) and photocatalytic activity, it is concluded that highest CCSD values do not result in largest photocatalytic efficiency.[9] A Russell-like mechanism similar to Scheme 1 is proposed to explain the experimental results. It is believed that O_2^- and $HOCH_2OO^{\bullet}$ are formed in close proximity on the catalyst surface upon UV irradiation. This process competes with electron−hole recombination, yielding highest rates of the photooxidation at small CCSD. The fact that the Russell-like mechanism requires the formation of the surface bound organotetraoxides species initiated by both photogenerated holes and electrons may explain the slower initial $CH_3O_{(a)}$ depletion rate in the presence of O_2 in the present study. It is noteworthy that photoreaction pathways and kinetics are under the influence of surface adsorption conditions. A recent study, reported by Schwitzgebel et al., has shown an alternative to the Russell-like mechanism in the photooxidation of C_8 organic compounds on a silicone-overcoated TiO_2 catalyst.[25] When chloride ions are excluded from the reaction zone by the covalently bound polymer, the C_8 photodecomposition proceeds via a current-doubling two-electron oxidation process.

The reaction pathways of the $CH_3O_{(a)}$ photodecomposition on TiO_2 in Scheme 1 are proposed to be initiated directly by photoholes. The photoreactions may be initiated by $OH^{\bullet}$ radicals. There is convincing evidence in the literature in support of $OH^{\bullet}$ radicals as initiating oxidants for photooxidation on TiO_2 surface.[26,27] However, in the diffuse reflectance flash photolysis study of several substrates/TiO_2 combinations, Draper et al. have not been able to detect any expected $OH^{\bullet}$ adduct intermediates.[28] This study strongly supports direct hole oxidation. The source of $OH^{\bullet}$ may come from hole-trapping of $H_2O_{(a)}$ or $OH_{(a)}$ groups. In the present study, the TiO_2 surface is free of water before UV irradiation, so the $OH^{\bullet}$ formation from H_2O is unlikely to occur. The other possible route is through $OH_{(a)}$ hole trapping. However, a recent ESR study of photolysis of hydrous TiO_2 colloids points out that the actual species formed from $OH_{(a)}$ decomposition is $-O^{\bullet -}$ whose chemical role is unknown.[10] Nonetheless, since $CH_3O_{(a)}$ is chemically bonded to the surface in the present study, it may effectively compete with any $OH_{(a)}$ to trap the photoholes diffusing to the surface, followed by decomposition to generate $-OCH_2^{\bullet}$ groups.

Conclusions

$CH_3O_{(a)}$ groups on TiO_2 undergo photooxidation initiated by hole-trapping to form $-OCH_2^{\bullet}$, which then further decomposes to generate $CH_2O_{(g)}$. The photoreaction rate is retarded by electron−hole recombination for prolonged UV irradiation. Adsorbed O_2 plays two roles: it recombines with $-OCH_2^{\bullet}$ and receives photoelectrons. In the presence O_2, the decomposition of $CH_3O_{(a)}$ on TiO_2 is most likely through the Russell-like mechanism to form adsorbed $HCOO_{(a)}$ and $H_2O_{(a)}$.

Acknowledgment. We gratefully acknowledge the support of the National Science Council of the Republic of China (Grant NSC-86-2113-M-006-014) for this research. We are grateful to Prof. S. W. Ho and Dr. J. C. Lin for informative discussions.

References and Notes

(1) Suda, Y.; Morimota, T.; Nagao, M. *Langmuir* **1987**, *3*, 99.
(2) Rossi, P. F.; Busca, G. *Colloids Surf.* **1985**, *16*, 95.
(3) Taylor, E. A.; Griffin, G. L. *J. Phys. Chem.* **1988**, *92*, 477.
(4) Hussein, G. A. M.; Sheppard, N.; Zaki, M. I.; Fahim, R. B. *J. Chem. Soc., Faraday Trans. 1* **1991**, *87*, 2655.
(5) Lusvardi, V. S.; Barteau, M. A.; Farneth, W. E. *J. Catal.* **1995**, *153*, 41.
(6) Carlson, T.; Griffin, G. L. *J. Phys. Chem.* **1986**, *90*, 5896.
(7) Ohtani, B.; Nishimoto, S.-I. *J. Phys. Chem.* **1993**, *97*, 920.
(8) Wang, C. M.; Heller, A.; Gerischer, H. *J. Am. Chem. Soc.* **1992**, *114*, 5230.
(9) Sadeghi, M.; Liu, M.; Zhang, T.-G.; Stavropoulos, P.; Levy, B. *J. Phys. Chem.* **1996**, *100*, 19466.
(10) Micic, O. I.; Zhang, Y.; Cromack, K. R.; Trifunac, A. D.; Thurnauer, M. C. *J. Phys. Chem.* **1993**, *97*, 13284.

(11) Basu, P.; Ballinger, T. H.; Yates, J. T., Jr. *Rev. Sci. Instrum.* **1988**, *59*, 1321.
(12) Wong, J. C. S.; Linsebigler, A.; Lu, G.; Fan, J.; Yates, J. T., Jr. *J. Phys. Chem.* **1995**, *99*, 335.
(13) Degussa Technical Bulletin Pigments Report No. 56, 1990; p 13.
(14) Woodruff, D. P.; Delchar, T. A. *Modern Techniques of Surface Science*; Cambridge University Press: 1986; p285.
(15) *Eight Peak Index of Mass Spectra*, 4th ed.; The Royal Society of Chemistry, 1991: Vol. 1, ISBN-0-85186-417-1.
(16) Lin, J.-L. Unpublished results.
(17) Gomes, W. P.; Freund, T.; Morrison, S. R. *J. Electrochem. Soc.* **1968**, *115*, 818.
(18) Herzberg, G. *Molecular Spectra and Molecular Structure: I, Spectra of Diatomic Molecules*, 2nd ed.; VNR: New York, 1950; p 446.
(19) Qin, D.; Chang, W.; Chen, Y.; Zhou, J.; Chen, Y.; Gong, M. *J. Catal.* **1993**, *142*, 719.
(20) Naccache, C.; Meriaudeau, P.; Che, M.; Tench, A. J. *Trans. Faraday Soc.* **1971**, *67*, 506
(21) Shultz, A.; Jang, W.; Hetherington, W. M.; Baer, D. R.; Wang, L.-Q.; Engelhard, M. H. *Surf. Sci.* **1995**, *339*, 114.
(22) Meriaudeau, P.; Vedrine, J. C. *J. Chem. Soc., Faraday Trans. 2* **1976**, *72*, 472.
(23) Lu, G.; Linsebigler A.; Yates, J. T., Jr. *J. Phys. Chem.* **1995**, *99*, 7626.
(24) Schwitzgebel, J.; Ekerdt, J.; Gerischer, H.; Heller, A. *J. Phys. Chem.* **1995**, *99*, 5633.
(25) Schwitzgebel, J.; Ekerdt, J. G.; Futoshi, S.; Lindquist, S.-T.; Heller, A. *J. Phys. Chem. B* **1997**, *101*, 2621.
(26) Fox, M. A.; Dulay, M. A. *Chem. Rev.* **1993**, *93*, 341.
(27) Hoffmann, M. R.; Martin, S. T.; Choi, W.; Bahnemann, D. W. *Chem. Rev.* **1995**, *95*, 69.
(28) Draper, R. B.; Fox, M. A. *Langmuir* **1990**, *6*, 1396.